



## Influence of TiO<sub>2</sub> Layer Thickness as Photoanode in Dye-Sensitized Solar Cells

M. Shirkavand<sup>1</sup>, M. Bavir<sup>2\*</sup>, A. Fattah<sup>3</sup>, H. R. Alaei<sup>4</sup>, M. H. Tayarani Najaran<sup>5</sup>

<sup>1</sup> Physics Department, Khayyam University, Mashhad, Iran

<sup>2</sup> Electrical and Computer Engineering Department, Semnan University, Semnan, Iran

<sup>3</sup> Faculty of Electrical Engineering and Robotic, Shahrood University of Technology, Shahrood, Iran

<sup>4</sup> Faculty of Physics, IAU Varamin-pishva Branch, Tehran, Iran

<sup>5</sup> Faculty of Physics, Ferdowsi University of Mashhad, Mashhad, Iran

**ABSTRACT:** Dye-sensitized solar cells (DSSCs) are categorized as some of the inexpensive thin-film solar cells. The basis and foundation of these cells is a semiconductor that consists of an electrolyte and a light-sensitive anode. Titanium dioxide (TiO<sub>2</sub>) is a semiconductor that plays the role of the anode and is the main constituent of these cells. In this paper, we have addressed the functionality and performance of TiO<sub>2</sub> films with the thicknesses of 2.96, 7.54 and 11.1 μm in DSSCs. The morphology, crystal structure, and the optical band gap are some of the effective elements on the electron transfer rate and recombination process in the TiO<sub>2</sub> film. When using TiO<sub>2</sub>, one must choose the optimum thickness to ensure optimal short-circuit current, open-circuit voltage and fill factor so that the cell can have the highest possible efficiency. Analysing the obtained characteristic curves, it is concluded that the efficiency of a cell with a 2.96 μm TiO<sub>2</sub> film is 4.2%; the efficiency of a cell with a 7.54 μm TiO<sub>2</sub> film is 5.54% and the efficiency of a cell with an 11.1 μm TiO<sub>2</sub> film is 6%. Also, analysing the EIS shows that the highest electron lifetime is 17 milliseconds which is obtained for the cell with an 11.1 μm TiO<sub>2</sub> film. The films of TiO<sub>2</sub> for each cell are provided by the doctor-blade deposition method and the dyes are deposited on their surface.

### Review History:

Received: 4 November 2018

Revised: 18 December 2018

Accepted: 6 February 2019

Available Online: 6 February 2019

### Keywords:

Dye-sensitized solar cell

Photoanode

TiO<sub>2</sub>

Thickness

Efficiency

### 1- Introduction

Sunlight which contains a surprisingly large amount of energy has been used traditionally by a human being in various conditions. Due to population growth and the increasing demand in developing countries, we are faced with a global rise in energy consumption. Therefore, substituting fossil fuels for renewable energy sources is one of the biggest challenges facing mankind [1-2]. DSSCs are considered as proper economic substitutions for p-n junction semiconductor photovoltaic cells. In silicon cells, light absorption and charge transfer are both performed by one material; however, in the electrochemical structure of DSSCs, these two processes are completely separated [3-4]. Light is absorbed by some types of molecules called dyes which are sensitive to the visible spectrum. These molecules are located on the surface of a semiconductor with a wide bandgap [5-6]. Charge separation on the surface takes place by the injection of the optically excited charges that exist in the dye into the conduction band of the semiconductor. The charges are transferred from the semiconductor's conduction band to the charge collector [7]. There are various nanostructures of oxide semiconductors for use in the optical electrode of DSSCs; each of which has its own pros and cons. These nanostructures are constructed in the form of nanoparticles, nanowires, nanotubes, nano-belts, and three-dimensional structures in the shape of flowers, stars, oxide masses, etc. [8-9]. One important merit of nanostructures is that they have a larger internal contact area in comparison with those materials that use solid structures. The nano dimensions of these structures can also be effective in the movement and transfer of charges. In a way that they

limit the mean free path of the electric charges so that they demonstrate different electrical properties. This property of nanostructures is called the quantum confinement effect. These nanostructures can also play an important role in the field of optical effects by creating photonic band gaps and light scattering. Efforts are still being made to achieve a structure with an optimal efficiency for dye-sensitized solar cells [10]. One important substance as a Nano-structure material used in DSSCs is the TiO<sub>2</sub>. Many studies regarding the TiO<sub>2</sub> usefulness have investigated the effect of its thickness variations on the cell efficiency. Those studies have shown that increasing the TiO<sub>2</sub> layer thickness leads to more absorption of pigment molecules which in turn means that more photons can be injected and more electrons can be excited. Meanwhile, this increment raises the gap between ITO and TiO<sub>2</sub> and as a result, the excited electrons take more time to reach the ITO. Thus, there is more time for the recombination process and thus electron injection rate for creating electricity current diminishes [11-12]. Nowadays there are numerous methods for controlling the TiO<sub>2</sub> layer thickness, e.g. spraying and spin coating. However, the most promising way in this regard is the doctor Blade's approach due to its lower cost and higher speed compared to similar methods [13]. In this paper, we have investigated the influence of TiO<sub>2</sub> film thickness as photoanode in DSSCs.

### 2- The Experimental

In order to confirm the microstructure of the titanium dioxide particles in the powder, a TEM image is prepared using a FEG CM200 transmission electron microscope. The study of the phase and the crystalline structure of the TiO<sub>2</sub> powder is conducted by a Philips pw3710 machine using the x-ray

Corresponding author, E-mail:

diffraction technique. The x-ray powder diffraction spectrum is provided in order to confirm the type and phase of the used powder. Figure 1 plots the x-ray spectrum of the TiO<sub>2</sub> nanopowder which matches the type and phase composition (rutile and anatase) mentioned in the datasheet of the powder.

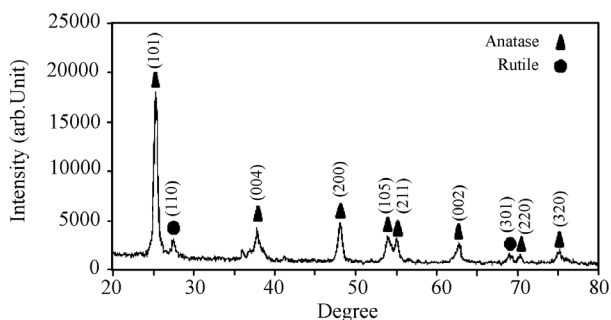


Fig. 1. X-ray diffraction spectrum of P-25 TiO<sub>2</sub> powder

### 2- 1- The Washing Procedures of FTO

- Washing with soap and water in an ultrasonic bath for 2 minutes
- Washing the substrate with deionized (DI) water
- Washing with 0.1 molar HCL in ethanol in an ultrasonic bath for 2 minutes
- Washing the substrate with DI water
- Washing with acetone in an ultrasonic bath for 2 minutes
- Washing the substrate with DI water
- Washing with ethanol in an ultrasonic bath for 2 minutes.

### 2- 2- Pretreatment

In order to prevent the recombination of the photoelectrons created in the TiO<sub>2</sub> with the FTO, a treatment is performed to form a 20 nm layer of TiO<sub>2</sub> on the FTO. First, a 2 molar solution must be prepared from pure TiCl<sub>4</sub> in deionized water. A 4°C ice/water bath is used in order to prepare this solution. All the containers must be completely dry during the operation. The reaction produces heavy steam; therefore, it must be conducted under a hood. The solution is transparent and must be kept in the freezer. The layers are placed in a 40 milli-molar TiCl<sub>4</sub> solution in DI water at a temperature of 70° C for 30 minutes. The 40 milli-molar solution is provided using the 2 molar solution which has been prepared earlier. Figure 2 shows the water bath for changing the temperature to the absorption process of the pigment of the layer.

### 2- 3- Deposition using doctor Blade's technique

Since there are various methods for the deposition of semiconductors and material choices as anodes, in this paper, the doctor Blade's method, which is common, commercial, and has a higher efficiency is incorporated. We place the layer on a plate; then apply calk or scotch tape on the FTO as shown in Figure 3. The surface we are working on should be larger than the final area of the cell.

We put the paste on one side of the FTO using a glass rod and spread it on the surface by a glass rod, a microscope slide or a Pasteur pipette.

In order to uniform the surface of the paste, we pour a few drops of ethanol vapor around the layer and cover it with a plate. The ethanol vapor uniform the layer. We dry the layer along with the tape around it at a temperature of 120°C in the oven for six minutes. The tape is not removed for the deposition of the subsequent layers. As described

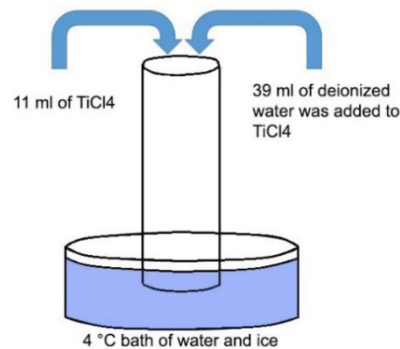


Fig. 2. Using a water bath for changing the temperature to absorption process of the pigment of layer

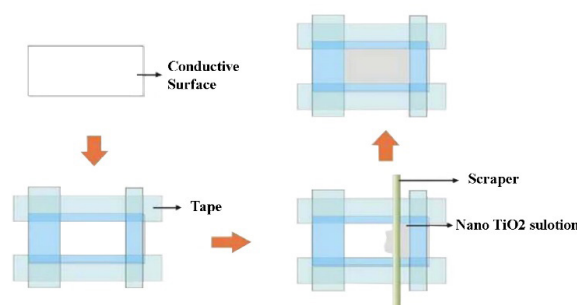


Fig. 3. Attach the FTO on the plate by Calc tape

above, we wait until the layer cools down; then we deposit the subsequent layers. Finally, at the end of the deposition process, we remove the tape from the surface.

### 2- 4- First sinter process

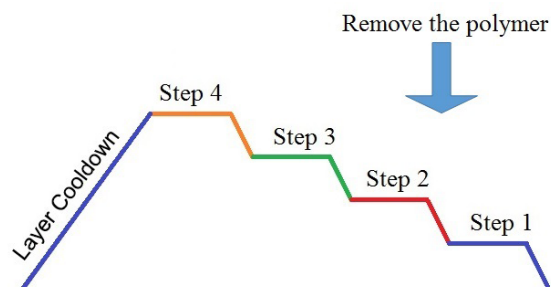


Fig. 4. Steps of heating the anode

In this stage, the layer is heated to a temperature of 500°C according to Figure 4.

Step 1: hold the paste until 325° C and after this stay for 10 minutes.

Step 2: hold the paste from 325° C until 375° C and after this stay for 10 minutes.

Step 3: hold the paste from 375° C until 450° C and after this stay for 15 minutes.

Step 4: hold the paste from 450° C until 500° C and after this stay for 30 minutes.

After the execution of the previous stages, the layer should be cooled down slowly; because a rapid change of temperature can cause cracks and it detaches the layer from its substrate. When the layers are heated, they should be scraped using a

lamella to reach the standard area of 0.25 cm<sup>2</sup>. In order to construct a dye-sensitized cell, the layer should be treated again using TiCl<sub>4</sub> after scraping.

#### 2- 5- The second sintering process

After the treatment, the layer is washed with DI water and ethanol and then heated for 30 minutes at a temperature of 500°C. When the temperature of the oven reaches 80°C, we place the layer in the dye solution.

#### 2- 6- Placing the Layer in the Dye Solution

When the samples are cooled down to a temperature of 80°C, they are placed in the dye at the same temperature. They remain in the dye solution at room temperature for 24 hours. In this project, the dye solution has a density of 0.5 millimolars.

The solvent can either be ethanol or acetonitrile/tert-butanol. In this project, we have used acetonitrile/tert-butanol as the solvent in order to prepare the 0.5 milli-molar dye solution.

#### 2- 7- The Preparation of the Cathode

After cutting a 1.5×1.5 piece of the substrate, we create a hole in the opposite electrode (the cathode) using a miniature milling machine in order to inject the electrolyte into the closed-cell. For this purpose, some holes or apertures should be embedded in the cathode. Using the miniature milling machine, we can create holes with diameters of 0.4 and 0.6 millimeters. The holes are embedded in the insulator side.

First, we heat the layers at a temperature of 460°C for 15 minutes. The purpose of this heating is to clean the surface. Then, we pour one drop of a 0.5 milli-molar solution of H<sub>2</sub>PtCl<sub>6</sub> on the FTO so that the whole surface is coated by the solution. Finally, we heat the layer again at 460°C for 15 minutes so that the platinum is fixed on the surface.

#### 2- 8- The Preparation of the Iodine-Based Electrolyte

The electrolyte of a granular DSSC is based on I<sup>-</sup>/I<sub>3</sub><sup>-</sup> redox pairs. To construct this electrolyte, we dissolve materials such as iodine ions in acetonitrile. The ionic liquid is used in order to stabilize the electrolyte. Electrolyte injection is performed using two different techniques: back vacuum filling and the simultaneous removal of the air. We will explain both of these methods in full detail in the following. In the back vacuum filling method -which is proper for smaller cells- the procedures of air evacuation and electrolyte injection are performed through an orifice. A hole with a diameter less than 0.5 mm is embedded on the active surface of the covered electrode. After completing the initial stages of sealing for the two electrodes constituting the cell, the hole on the platinum electrode is covered with a surlyn film and then sealed with thermal methods. After that, a needle is used to create a hole in the orifice on the film and a drop of electrolyte is poured on it. We put the cell inside a vacuum chamber. When suction begins, the air inside the cell starts to clear out; and with the sudden release of the air valve, the electrolyte is sucked into the space between the two electrodes. In the method of the simultaneous removal of air for electrolyte injection, all stages are similar to the previous method. The difference is that two holes are created on the platinum electrode which are approximately 5 mm apart. The electrolyte is injected into one of the holes and the air in the cell is cleared out of the other one. After the injection process is complete, these two

holes are sealed in the same manner. In this project, we have used a single orifice cathode in order to ensure small sizes for the cells. Figures 5 and 6 show the before and after sealing.

#### 2- 9- Sealing and Closing Cell Components

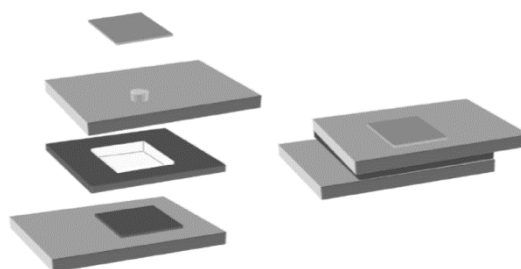


Fig. 5. Left hand- the components of one hole-type cell before final sealing Right hand -sealed cells

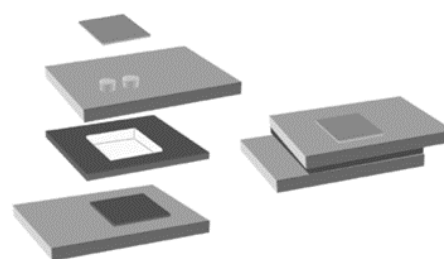
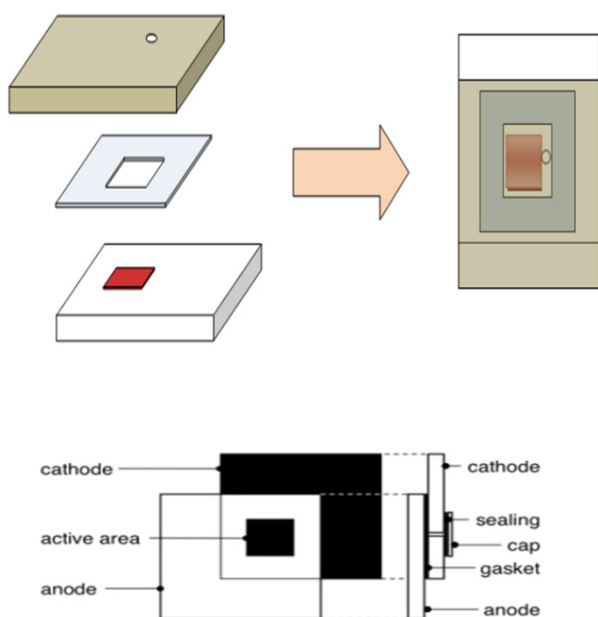


Fig. 6. Left hand: components of two holes-type cell before final sealing, right hand: sealed cells

Due to the extremely high corrosion of an electrolyte that contains iodine and acetonitrile, choosing a proper material for sealing is inevitable in order to prevent the evaporation of the electrolyte and the formation of a short circuit between the photo-electrode and the platinum electrode. The sealing process is performed using a 30 μm layer of Surlyn, which is the industrial name of a thermoplastic polymer composite from the Dyesol Company. The softening point of this material is below 100°C, and the recommended temperature for the sealing stage is between 110°C to 130°C. The reversible viscosity of thermoplastic materials reduces by the rising of the temperature; thus, a thorough sealing is achieved with this method. It is necessary to consider the parameters of time, temperature, and the applied pressure in order to achieve optimum sealing. For this purpose, the temperature of the oven is set to 130°C and the pressure conditions are applied to both electrodes using two metal clamps; then, the electrodes are heated for 15 to 17 minutes. Due to the difference between the thermal capacity of the air inside the oven and the cell and also the time it takes for the temperature of the sealing cell to reach the temperature of the oven, the temperature of the cell should be controlled by a separate thermometer. A Fluke 289 multi-meter equipped to a K-type thermocouple with a resolution of 0.1°C is used in order to evaluate and maintain the temperature of electrodes in the melting temperature of the sealant.

First, we cut a polymer with the commercial name of Surlyn using a stencil.

Then, we wash the polymer with ethanol and place it between the anode and the cathode as described in the following. Figure 7 portrays the schema of the preparation of DSSC based on titanium dioxide.



**Fig. 7. The schema of preparation of DSSC based on titanium dioxide**

The cell position is fixed by using metal clamps and is put under pressure and then is made hot at a temperature of 120°C for 90 seconds. The polymer melts and the cell is prepared for electrolyte injection.

It is recommended to use a single orifice cathode for the injection process, which leads to a higher stability rate for the cell. In the case of the single orifice cathode, we should use a vacuum to fill the electrolyte.

In most cases, a double orifice cathode is used which can be filled without any need for vacuum and does not impair the cell function.

#### 2- 10- Images of Scanning Electron Microscope (SEM)

The UV-visible spectrum of the layers before and after the deposition of the dye coating is used in order to study the connection and the reaction of the dye and the surface of titanium dioxide. This spectrum is prepared using the Perkin Elmer Lambda-25 device in the range of 400 to 600 nm which contains the absorption peaks of the dye.

The constructed cells are placed under a light with an intensity of 100 mw/cm<sup>2</sup> for 3 hours. The light intensity is measured using Solar Meter Mod.776 and a water filter is used in order to remove the infrared part of the radiation. The filter is used until the voltage and current reach a steady state, and so the cell is prepared for the tests during radiation.

As seen in Figure 8, the particle-size distribution has an average value of 20 to 25 nm. In addition, the morphologies of the powder particles are nearly spherical and uniform.

The SEM images of the deposited layers are provided in order to ensure there are no cracks in the layer and also to observe the surface microstructure. The SEM images of the titanium dioxide layer are plotted for three thicknesses of 2.96, 7.54 and 11.1 μm and with the magnifications of 10000x, respectively. As seen in the Figures 9,10, and 11, no cracks are visible in the deposited layers. It is also evident that

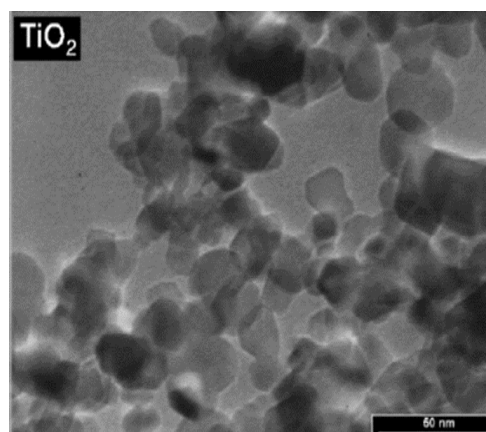


**Fig. 8. The image of the transmission electron microscope of nano-powder of titanium dioxide**

the cohesion and density of the layers increase by executing thermal operations and increasing the thickness of the porous layers. The SEM images of the layers indicate that these surfaces have a slight difference in terms of the number of vacancies, the agglomerate structure, and the number of grain boundaries. All these characteristics affect the speed and path of the electron movement on the surface of the electrode.

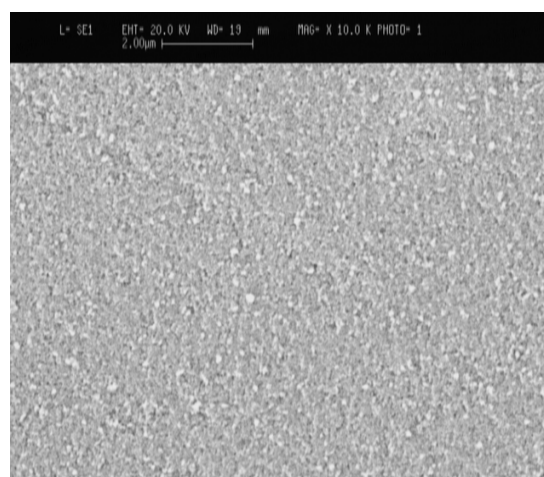


**Fig. 9. The image of the scanning electron microscope of the surface of covered titanium dioxide layer using the doctor blade method with a thickness equal to 2.96 μm at 10000× magnification.**

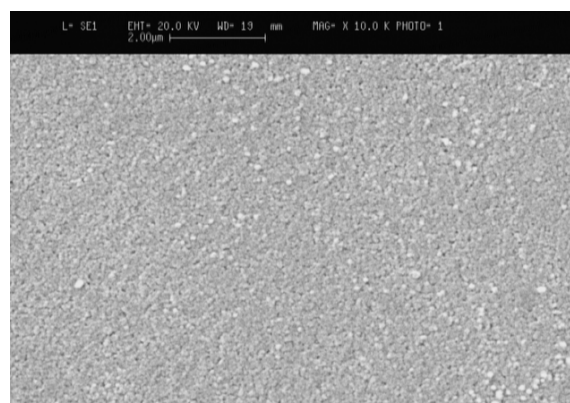


**Fig. 10. The image of the scanning electron microscope of the surface of covered titanium dioxide layer using the doctor blade method with a thickness of 7.54 μm at 10000× magnification**

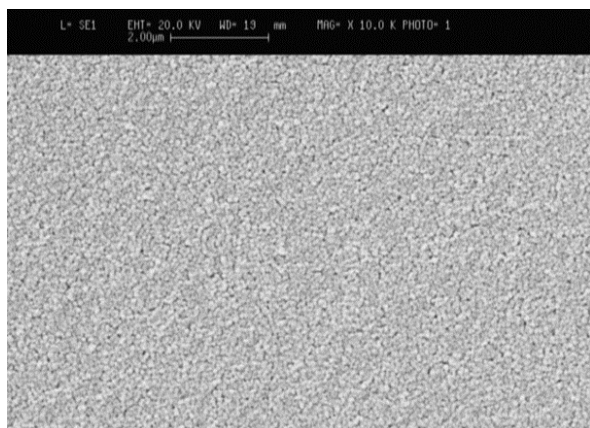


**Fig. 11. The image of the scanning electron microscope of the surface of covered titanium dioxide layer using the doctor blade method with a thickness of 11.1 μm at 10000× magnification**

### 2- 11- Deposition of Platinum

Deposition of platinum is performed using two methods. The first is to pour a drop of hexachloroplatinic acid on the substrate and the second is to prepare and apply a platinum paste. The inadequate microscopic quality and the macroscopic heterogeneity of the deposition on the surface leads us to consider using an alternative method with the purpose of resolving these two problems. The main reason of

using a polymer composite for the deposition of platinum is to reduce the mobility of the platinum precursor which leads to the doping of the precursor in the evaporation centers and thus the heterogeneity of the coating process. This heterogeneity -which is also visible in the macroscopic scale- reduces the performance as well as diminishing the aesthetic appeal of the cell. Increasing the viscosity of the precursor composition is an adequate solution to this problem which can be achieved by using a platinum paste. Experience suggests that the two features necessary for producing a suitable platinum paste are the platinum to polymer ratio and the viscosity of the paste. A platinum paste is actually a polymer gel and the final platinum layer is produced in three stages. The first stage involves the evacuation of the liquid component, which in this case is isopropanol. In the second stage, the polymer environment is cleared out and in the third stage -which thermally overlaps the second stage- the platinum precursor is calcined and the platinum remains on the surface. It is evident that the isopropanol is cleared out at a temperature between 80°C and 90°C, which leads to an endothermic reaction at a central temperature of about 83°C. Note that this temperature differs from the boiling temperature of isopropanol only by 0.5°C. There are also two exothermic peaks with central temperatures of 342°C and 366°C between the temperatures of 340°C and 400°C. These peaks represent the decomposition of polyethylene glycol and hexachloroplatinic acid. After performing the deposition by applying the paste, the images

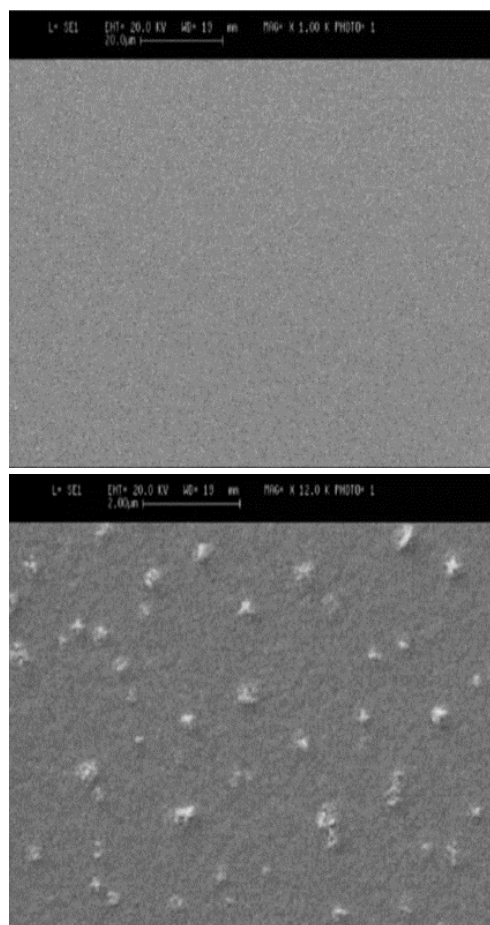


**Fig. 12. The image of the scanning electron microscope of the surface of the deposited platinum layer using platinum paste method at the magnification of a: 1000 and b:12000 times**

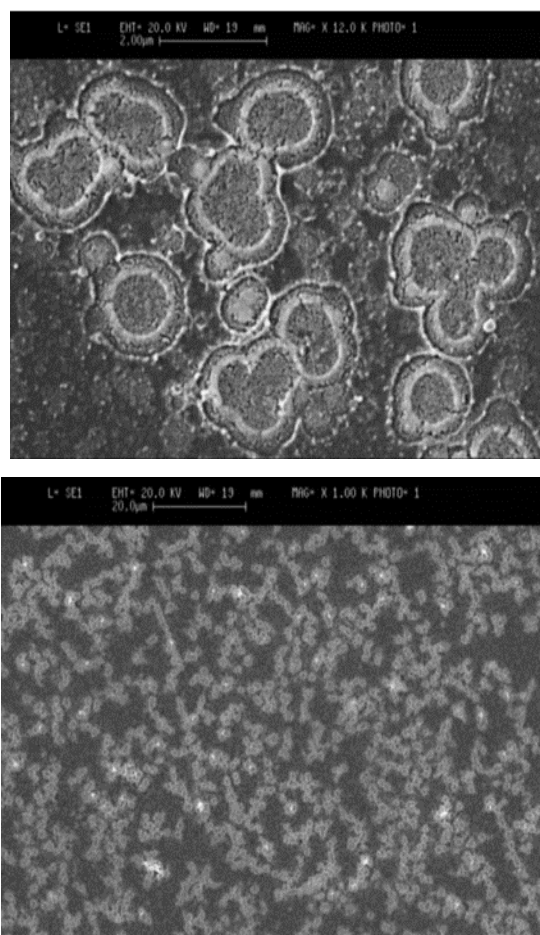


**Fig. 13. The image of scanning electron microscope of the surface of the deposited platinum layer using dropping drop method at the magnification of a: 1000 and b:12000 times**

of the scanning electron microscope are prepared. These two images are plotted in Figures 12 and 13 with magnifications of 1000x and 12000x, respectively. It is evident in the figures that there are no heterogeneities in the layer deposited by the first method. Also, a lower amount of platinum is used and a more desirable macroscopic appearance is achieved.

## 2- 12- The image of the scanning electron microscope of the cross-section

In order to measure the thickness of the porous layers by cutting the anode through the middle, we used Scanning Electron Microscopy. Figures 14, 15, and 16 display the images of scanning electron microscope of the cross-section area of the anode with the coating of TiO<sub>2</sub> porous layer with a thickness of 2.96 μm, 7.54 μm and 11.1 μm.

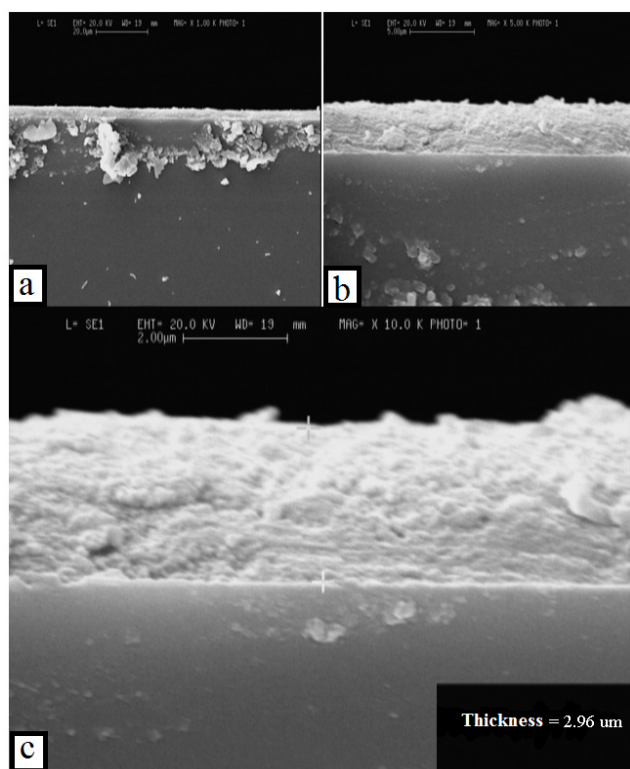


**Fig. 14. The images of scanning electron microscope of the cross-section area of the anode with the coating of TiO<sub>2</sub> porous layer with a thickness of 2.96 μm at a: × 1000 magnification. b: × 5000 magnification**

## 2- 13- Sealing

The diagram of the changes in the cell temperature as a function of time is plotted in Figure 17. The temperature is measured by a Fluke 289 multi-meter equipped with a K-type thermocouple with a resolution of 0.1°C. According to the diagram, the temperature of the electrodes reaches the lower limit of the recommended temperature for sealing (110°C) in 6 minutes and the upper limit (130°C) in about 17 minutes. Since the optimality of the sealing is evaluated visually, the best approach for determining the final time is trial and error. According to the conducted experiments, a time range of 15 to 17 minutes is sufficient if the above conditions are considered for temperature and pressure.

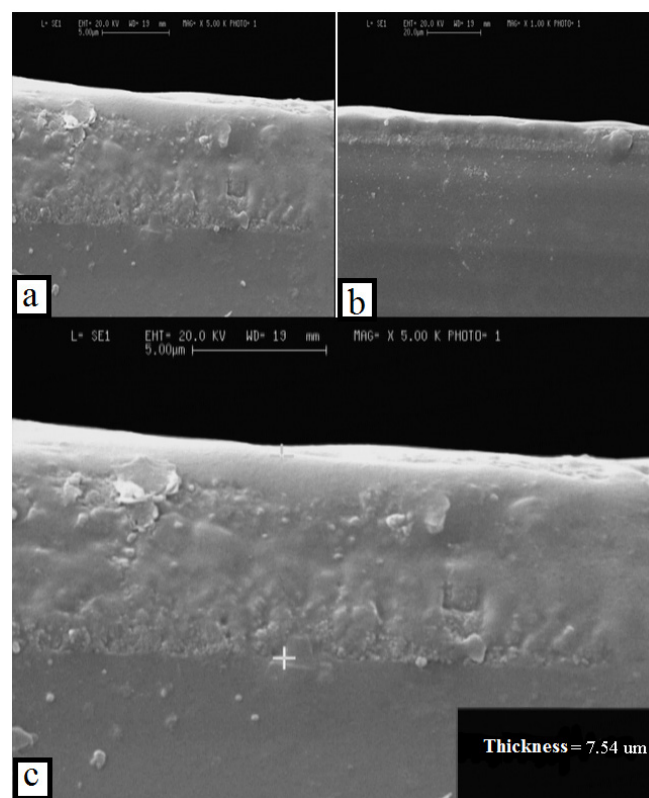


**Fig. 15. The images of scanning electron microscope of the cross-section area of the anode with the coating of TiO<sub>2</sub> porous layer with a thickness of 7.54 μm at a: ×1000 magnification, b: ×5000 magnification. c: ×10000 magnification**

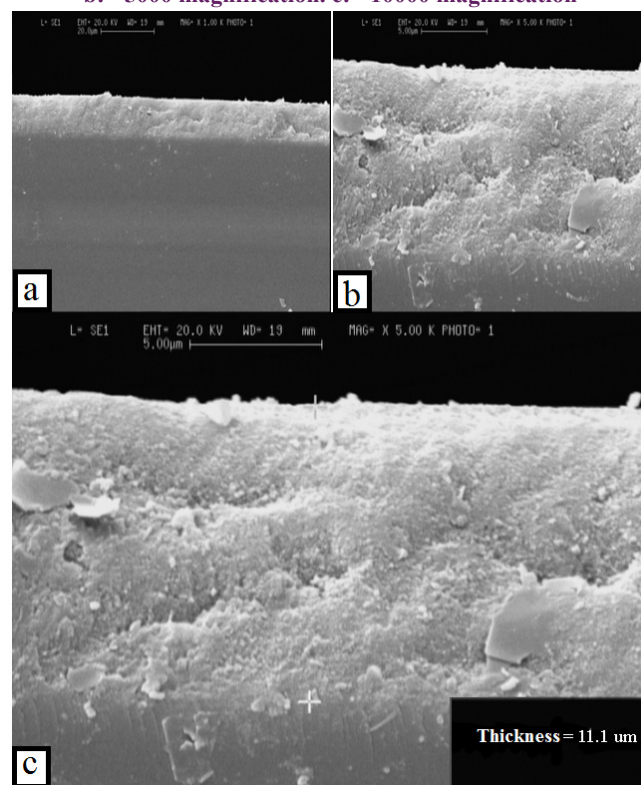


**Fig. 16. The images of scanning electron microscope of the cross-section area of the anode with the coating of TiO<sub>2</sub> porous layer with a thickness of 11.1 μm at a: × 1000 magnification. b: × 5000 magnification. c: × 10000 magnification**

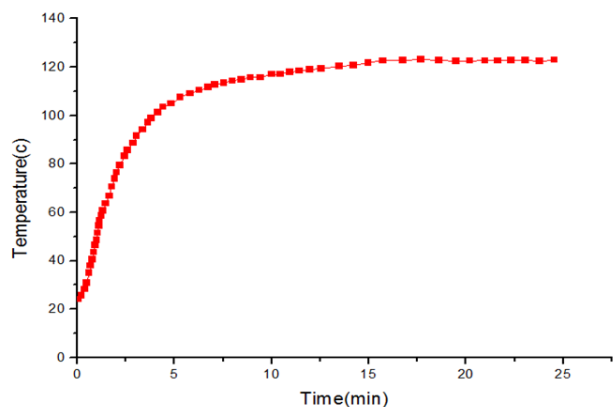


Fig. 17. Temperature-time curves of sealed cell in an oven with a temperature of 130°C

### 3- Characteristic diagram of the current-voltage of cells

Some information, including the open-circuit voltage ( $V_{oc}$ ), the short-circuit current ( $J_{sc}$ ), the fill factor (FF) and the efficiency of each cell is obtained using this test. By analyzing the results and the current-voltage test, we can conclude that the efficiency of the cells is affected by the physical properties of the surface such as the thickness, coarseness, roughness, the number of vacancies and the agglomeration rate of the surface. Table 1 shows the performance of DSSCs with different thicknesses.

Table 1. Performance of DSSCs made using photoanodes of TiO<sub>2</sub> at different thicknesses

thickness ( $\mu\text{m}$ )	$V_{oc}$ (mV)	$J_{sc}$ ( $\text{mA Cm}^{-2}$ )	FF	$\eta$ (%)
2.96	700	8.57	0.7	4.2
7.54	695	11.58	0.6	5.4
11.1	675	13.51	0.6	6.0

The photo-electrode with a thickness of 11.1  $\mu\text{m}$  demonstrates the best performance in terms of conversion efficiency and the highest short-circuit current density. Also, the 15  $\mu\text{m}$  photo-electrode displays the highest open-circuit voltage and the lowest short-circuit current, fill factor and efficiency. Therefore, the ideal thickness for this paste is 11-12  $\mu\text{m}$ . The short-circuit current drops drastically for thicknesses greater than 12  $\mu\text{m}$ ; which is caused by an increase in the recombination rate in the cells. In Figure 18, the I-V curve of DSSCs that include photo-anodes made of porous layers of TiO<sub>2</sub> with various thicknesses is illustrated.

As Figure 19 shows, by increasing the thickness of photo electrode, the fill factor of the cells is reduced. In fact, the process of recombination in the cells is increased by increasing the film thickness of titanium dioxide. On the other hand, in photoanode, it occurs at the lowest thickness of the recombination process. The best efficiency and performance for the cells made by the technique of deposition of the doctor blade is related to the thickness of about 11.1  $\mu\text{m}$  that this thickness is considered as the optimum thickness by taking into account the principles of making and preparing and deposition technique.

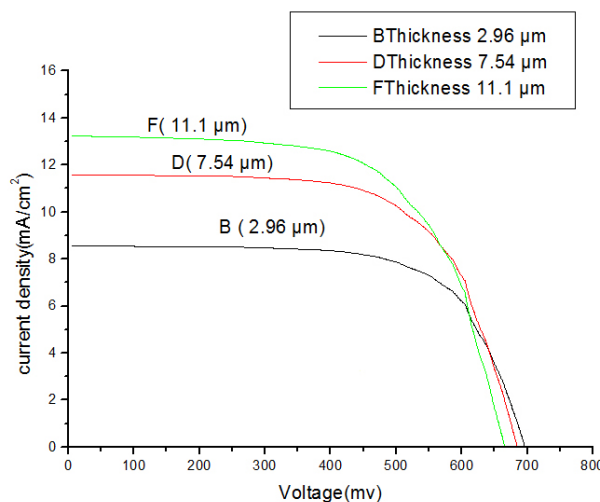


Fig. 18. current-voltage curves of solar cells made by anodes with the thickness of 11.1-F, 7.54-D, 2.96-B  $\mu\text{m}$

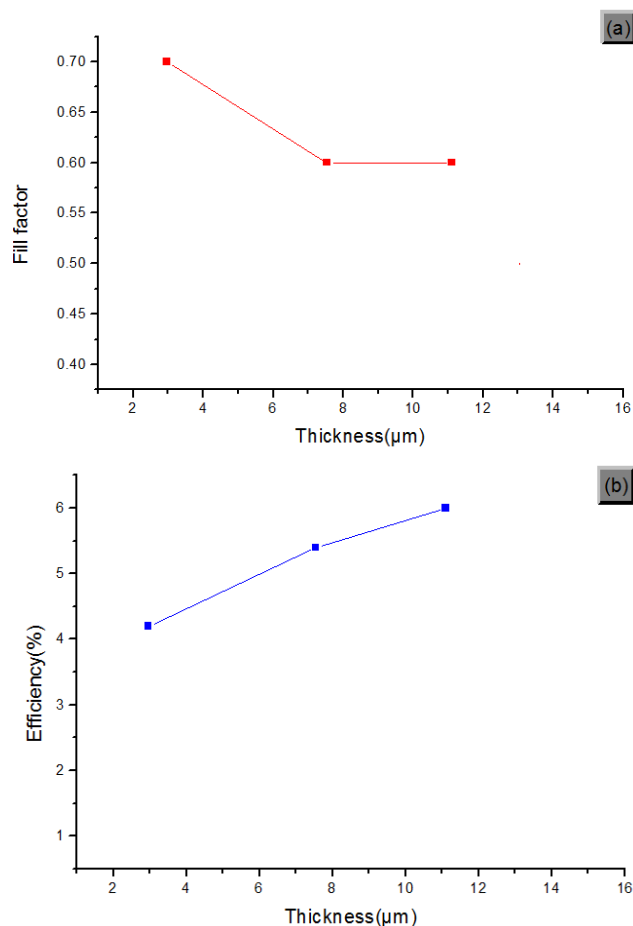


Fig. 19. a: Variation of fill factor, b: efficiency versus film thickness of TiO<sub>2</sub>

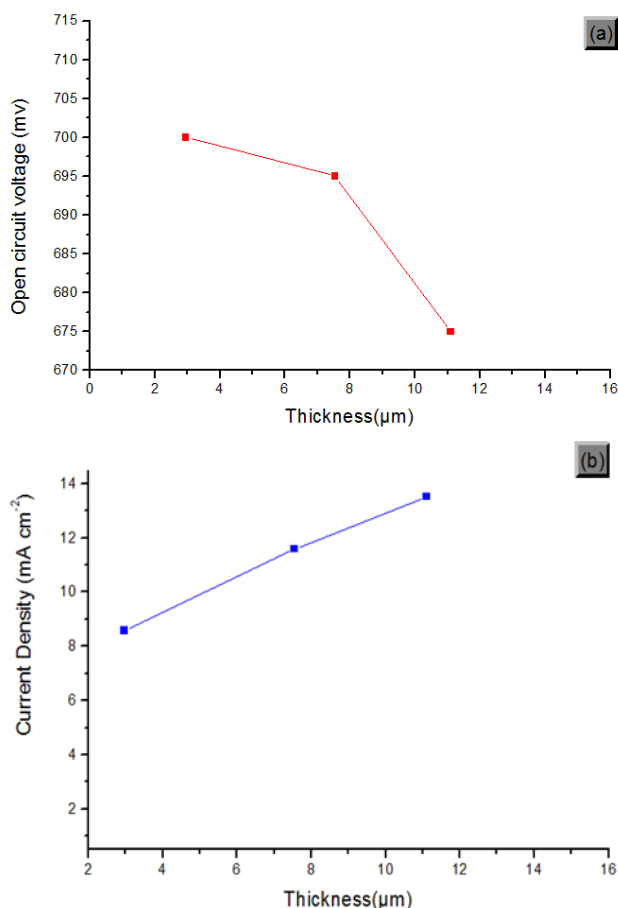


Fig. 20. a: Variation of open-circuit voltage, b: short-circuit current versus film thickness of TiO<sub>2</sub> in photoanodes

Figure 20 shows a) the variation of open-circuit voltage b) short-circuit current versus thickness of the porous film of TiO<sub>2</sub> in photoanodes. By increasing the thickness of the porous layers, short-circuit current and open-circuit voltage are increased.

**4- The study of the effect of the layer thickness of TiO<sub>2</sub> on the physical properties of cells made by Electrochemical Impedance Spectroscopy (EIS) method**

In order to understand better the effects of the layer thickness on the performance of the DSSC, electrochemical impedance spectroscopy is performed for the cells. The important parameters of the cells such as the chemical capacity (C<sub>μ</sub>) and the charge transfer resistance (R<sub>ct</sub>) are obtained by modeling the experimental results of the impedance using the equivalent electric circuit of the cells.

In Figure 21, the diagrams obtained by measuring the impedance of the cells constructed with different thicknesses of titanium dioxide are illustrated. In this case, the impedance spectrum of all the cells is measured by a solar simulator when exposed to light radiation of 1.5 AM in the frequency range of 1 kHz to 0.1 Hz.

The charge transfer resistance (R<sub>ct</sub>) for the constructed cells is derived using the equivalent circuit and the results of the impedance. In Figure 22 the resistances of the equivalent circuit of the cells are given. R<sub>s</sub> is the resistance of the FTO; R<sub>ct1</sub> is the resistance of the platinum electrode and R<sub>ct2</sub> is the charge transfer or charge recombination resistance.

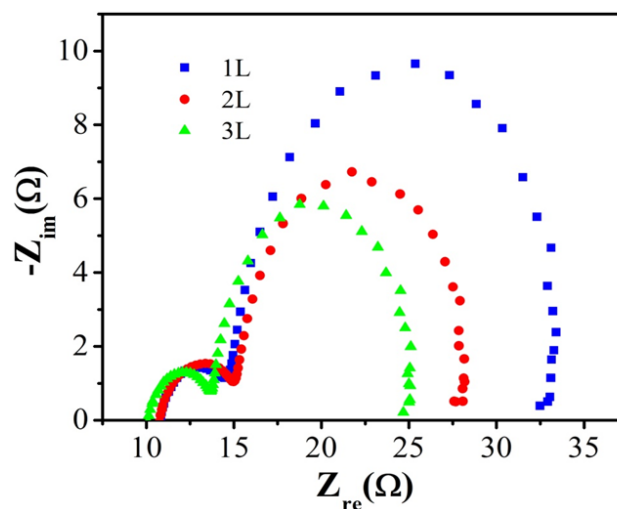


Fig. 21. Impedance spectra of DSSC prepared, experimental data and EIS model

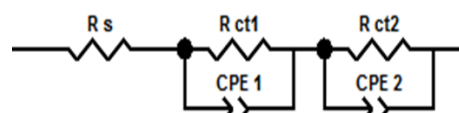


Fig. 22. The used equivalent circuit to obtain resistance of charge transfer in DSSC charge

Table 2. Resistances obtained for cells made by the equivalent circuit of Fig. 22

thickness (μm)	The maximum frequency	C <sub>μ</sub> (103μF/cm <sup>2</sup> )	R <sub>s</sub> (Ω)	R <sub>ct1</sub> (Ω)	R <sub>ct2</sub> (Ω)
2.96	12.24	2.74	10.77	4.06	4.95
7.54	10.96	4.64	10.73	4.62	3.26
11.1	9.36	5.90	10.07	3.85	2.85

The charge transfer resistance reduces by increasing the thickness of the TiO<sub>2</sub> layer. Since charge transfer resistance is dependent on the density of electrons in the nanostructure, the charge density in the structure is increased by increasing the layer thickness. The resistances of the FTO and the platinum are independent of the layer thickness which can also be seen in the data above. As the production rate of the photoelectrons increases, the chemical potential is also increased. These conditions are provided by increasing the thickness of the layer. This procedure can be observed in the above table. Increasing the thickness of the layer also increases electron lifetime; which means that the recombination rate of the electrons has decreased. This procedure can be justified as follows: the electrons are quickly directed into the nanostructure by increasing the thickness; therefore, they move away from the electrolyte boundary. This transfer reduces the recombination rate of the electrons and improves the electron collection efficiency.

The average lifetime of an electron in a photo-electrode structure is calculated by the following equation:

In this equation, F<sub>max</sub> is the frequency corresponding to the maximum in the middle arch of the Bode plot. The Electron

lifetime corresponding to the maximum in the middle arch of the Bode plot is given in Table 3 for the cells constructed by titanium dioxide. Since the lifetime in the structure is a criterion of the recombination rate of the electrons injected into the conduction band of the photo-electrode and the oxidized ions in the electrolyte, it can be concluded that the electron lifetime rises by increasing the layer thickness. In other words, the recombination rate of the electrons reduces.

**Table 3. Electron lifetime of cells made at different thicknesses**

Thickness ( $\mu\text{m}$ )	Electron lifetime (msec)
2.96	13
7.54	15
11.1	17

This is the concentration of the energy traps in the conduction layer which is responsible for the current transfer. A higher concentration of energy traps leads to skips and thus more barriers in the electron movement.

### 5- Conclusion

According to the obtained current-voltage curves, the following results can be concluded. The cell with the 2.96  $\mu\text{m}$   $\text{TiO}_2$  film has an open-circuit voltage of 700 millivolts, a short-circuit current of 8.57 milli-amperes, a fill factor of 70% and an efficiency of 4.2%. The charge transfer resistance for this cell is 4.95 ohms and the electron lifetime is calculated to be 13 milliseconds. As the thickness of the  $\text{TiO}_2$  film is increased from 2.96 to 7.54  $\mu\text{m}$ , the obtained open-circuit voltage decreases to 695 millivolts, the short-circuit current increases to 11.58 milli-amperes. Moreover, the fill factor decreases to 60% and the cell efficiency reaches 5.4%. Analyzing the electrochemical impedance shows a charge transfer resistance of 3.26 ohms and an electron lifetime of 15 milliseconds for this cell. If we change the thickness of the  $\text{TiO}_2$  film to 11.1  $\mu\text{m}$ , we obtain an open-circuit voltage of 675 millivolts, a short-circuit current of 13.51 milli-amperes, a fill factor of 0.6 and an efficiency of 6%. Also, the obtained electron lifetime for this cell is 17 milliseconds and the charge transfer resistance is equivalent to 2.85 ohms. It is evident that the electron lifetime lowers in the cell with the 11.1  $\mu\text{m}$   $\text{TiO}_2$  film; which means that the electron recombination has decreased, resulting in the increase of the short-circuit current. On the other hand, the charge transfer resistance is inversely proportional to electron density in the nanostructure; and the increase of electron density due to the decrease of recombination has led to a decrease in the charge transfer resistance in the cell with the 11.1  $\mu\text{m}$  film. Thus, this cell has the highest efficiency which is 6%.

### References

[1] A. Hagfeldt, G. Boschloo, L. Sun, L. Kloo, H. Pettersson, Dye-sensitized solar cells, *Chemical reviews*, 110(11)

(2010) 6595-6663.

- [2] D. Kuang, C. Klein, S. Ito, J.E. Moser, R. Humphry-Baker, N. Evans, F. Durrant, C. Graetzel, S.M. Zakeeruddin, M. Grätzel, High-efficiency and stable mesoscopic dye-sensitized solar cells based on a high molar extinction coefficient ruthenium sensitizer and nonvolatile electrolyte, *Advanced Materials*, 19(8) (2007) 1133-1137.
- [3] R. Cisneros, M. Beley, J.-F. Fauvarque, F. Lapique, Investigation of electron transfer processes involved in DSSC's by wavelength dependent electrochemical impedance spectroscopy ( $\lambda$ -EIS), *Electrochimica Acta*, 171 (2015) 49-58.
- [4] M. Bavir, A. Fattah, An investigation and simulation of the graphene performance in dye-sensitized solar cell, *Optical and Quantum Electronics*, 48(12) (2016) 559.
- [5] R. Cisnerosa, M. Beleyb, F. Lapique, Electrochemical Impedance Model of a (Low-cost) Dye-Sensitized Solar Cell, *CHEMICAL ENGINEERING*, 41 (2014).
- [6] S. Sarker, H.W. Seo, D.M. Kim, Electrochemical impedance spectroscopy of dye-sensitized solar cells with thermally degraded N719 loaded  $\text{TiO}_2$ , *Chemical Physics Letters*, 585 (2013) 193-197.
- [7] J. Bisquert, F. Fabregat-Santiago, Impedance spectroscopy: a general introduction and application to dye-sensitized solar cells, in: *Dye-sensitized solar cells*, EPFL Press, (2010) 477-574.
- [8] M. Grätzel, Solar energy conversion by dye-sensitized photovoltaic cells, *Inorganic chemistry*, 44(20) (2005) 6841-6851.
- [9] L.M. Gonçalves, V. de Zea Bermudez, H.A. Ribeiro, A.M. Mendes, Dye-sensitized solar cells: A safe bet for the future, *Energy & Environmental Science*, 1(6) (2008) 655-667.
- [10] M. Nirmal, L. Brus, Luminescence photophysics in semiconductor nanocrystals, *Accounts of chemical research*, 32(5) (1999) 407-414.
- [11] B. Ferreira, D. Sampaio, R.S. Babu, A. de Barros, Influence of nanostructured  $\text{TiO}_2$  film thickness in dye-sensitized solar cells using naturally extracted dye from *Thunbergia erecta* flowers as a photosensitizer, *Optical Materials*, 86 (2018) 239-246.
- [12] J. Kumari, N. Sanjeevadarshini, M. Dissanayake, G. Senadeera, C. Thotawatthage, The effect of  $\text{TiO}_2$  photo anode film thickness on photovoltaic properties of dye-sensitized solar cells, *Ceylon Journal of Science*, 45(1) (2016).
- [13] M.E. Yeoh, K.Y. Chan, H.Y. Wong, Investigation on the Thickness Effect of  $\text{TiO}_2$  Photo-Anode on Dye-Sensitized Solar Cell Performance, in: *Solid State Phenomena, Trans Tech Publ*, (2018) 76-80.

Please cite this article using:

M. Shirkavand, M. Bavir, A. Fattah, H. R. Alaei, M. H. Tayarani Najaran, Influence of  $\text{TiO}_2$  Layer Thickness as Photoanode in Dye-Sensitized Solar Cells, *AUT J. Elec. Eng.*, 51(1) (2019) 101-110.

DOI: 10.22060/ej.2019.15241.5254



